

**Measurement of x-ray multielectron photoexcitations at the I<sup>-</sup> K edge**Paola D'Angelo,<sup>\*</sup> Andrea Zitolo, Valentina Migliorati, and Nicolae Viorel Pavel*Dipartimento di Chimica, Università di Roma "La Sapienza", P. le A. Moro 5, 00185 Roma, Italy*

(Received 22 July 2008; revised manuscript received 17 September 2008; published 13 October 2008)

We report the direct measurement by x-ray-absorption spectroscopy of the complete spectrum of multielectron excitations at the I<sup>-</sup> K edge. The photoabsorption cross section of crystalline tetramethylammonium iodide was measured at 28, 50, and 150 K, and room temperature. The latter spectrum has been found to be largely dominated by the opening of multielectron excitation channels, thus providing a very good model of the I<sup>-</sup> atomic background which can be used in the analysis of ionic iodine compounds. Features due to the simultaneous excitations  $1s5p$ ,  $1s5s$ ,  $1s4d$ ,  $1s4p$ ,  $1s4s$ ,  $1s3d$ , and  $1s3p$  have been recognized, and their identification is supported by previous experimental and theoretical determinations on Xe and HI.

DOI: [10.1103/PhysRevB.78.144105](https://doi.org/10.1103/PhysRevB.78.144105)

PACS number(s): 32.30.Rj, 32.80.Fb, 33.20.Rm, 87.64.kd

**I. INTRODUCTION**

X-ray photoabsorption spectra have generally been interpreted in the framework of the one-electron approximation. However, the existence of the multielectron excitation process, where the removal of a core electron by photoabsorption causes excitation or ionization of additional electrons from shallower orbitals of the same atom, has been known in x-ray-absorption spectroscopy (XAS) for a long time.<sup>1</sup> The experimental determination of the complete spectrum of multielectron photoexcitations can be performed only for monoatomic gases<sup>2-14</sup> and vapors of metals.<sup>15,16</sup> In solid, liquids, and even molecular gases, the weak multielectron features are usually masked by the much larger x-ray-absorption near-edge structure (XANES) and extended x-ray-absorption fine structure (EXAFS) dominating the spectrum in this energy range.<sup>17-20</sup> While the structural contribution to the absorption cross section can be properly calculated for a known arrangement of atoms, the multielectron excitation signal is not predictable with comparable precision. Therefore, the presence of double-electron excitations can hamper a proper extraction of the structural parameters from the XAS spectra even if their intensity is usually only a few percent of the single-electron transition. This is especially true for disordered systems, such as solutions, where the structural oscillations are usually weak.<sup>20,21</sup> There is a high interest in the study of solvated atomic ions as a means of understanding the details of solvation dynamics and hydration processes,<sup>22-24</sup> and it is important, for this purpose, to disentangle the multielectronic contributions from the structural ones.

While detailed investigations on the multielectronic excitations at the K shell of the bromide ion have been carried out,<sup>18,25,26</sup> there exists to our knowledge no such study on the iodide ion. On the other hand, several investigations have been devoted to the study of multielectron transition processes in the x-ray-absorption spectra of the Xe atom (which is isoelectronic with I<sup>-</sup>) both at the K and L edges.<sup>7-9,12-14</sup> Also, Buontempo *et al.*<sup>27</sup> carried out the analysis of the double-electron excitation channels above the I K edge using the absorption spectrum of the HI and I<sub>2</sub> molecules in the gas phase. Several anomalies were identified and assigned to the additional excitations of fourth shell electrons, in particular

$4d$ ,  $4p_{3/2}$ , and  $4p_{1/2}$ . In addition, clear slope changes were detected in the EXAFS region around 640 and 960 eV associated with additional excitations of  $3d$  and  $3p$  electrons, respectively. A model accounting for this complex background was developed for HI and was transferred to the absorption spectra of I<sub>2</sub> molecules either isolated or embedded in a condensed medium.<sup>27</sup> The correctness of this procedure was investigated in a study on bromine<sup>28</sup> in which it was shown that the transferability of the atomic background of an element is limited to a very narrow class of compounds, where the photoabsorber atom has the same oxidation state and a similar chemical environment. This applies especially for the valence excitations occurring in the XANES region that are strongly affected by the bonding of the element to its neighbors and its oxidation state. Conversely, for deep double-electron excitations which do not change appreciably with the environment, it is possible to define a transferable atomic background that can be used to extract, with improved accuracy, the EXAFS signal of systems containing a given photoabsorber.

A model atomic background for iodine was also determined by Gomilšek *et al.*<sup>29</sup> using silica-based nanocomposite redox I<sup>-</sup>/I<sup>3-</sup> electrolytes, and the  $1s4d$ ,  $1s4p$ , and  $1s3d$  multielectron photoexcitations were extracted from the raw data by subtracting the EXAFS structural oscillation.

In the present paper we report the direct measurement of the complete spectrum of multielectron excitations at the I<sup>-</sup> K edge. In order to obtain the pure atomic spectrum, we have selected a compound, crystalline tetramethylammonium iodide (TMAI), where the I<sup>-</sup> ions are only weakly bound to the surrounding species. Indeed, in this compound the I<sup>-</sup> ions are surrounded only by hydrogen atoms in the first coordination shell, presenting an almost negligible structural contribution at room temperature. With this study we intend to perform a direct experimental determination of the atomic background of I<sup>-</sup>, which can be used in the analysis of its XANES and EXAFS spectra in water or organic solvents.

**II. EXPERIMENTAL SECTION**

The experiment has been performed at the BM29 beamline at the European Synchrotron Radiation Facility (ESRF).<sup>30</sup> The monochromator was equipped with two flat

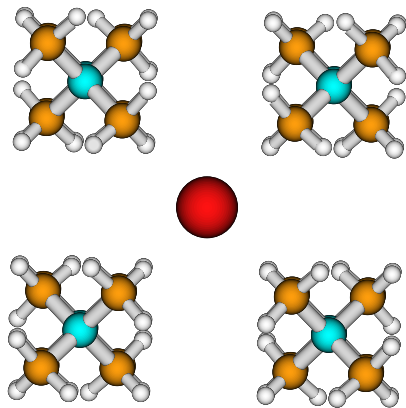


FIG. 1. (Color online) Perspective view of the TMAI crystalline structure.

Si(511) crystals for high-energy operation with an energy resolution of about 2 eV at 33.0 keV. In order to reduce harmonic contamination, which is weak in any case at the I  $K$  edge, the crystals were kept slightly detuned with a feedback system. The incident and transmitted fluxes were monitored by ionization chambers filled with Kr gas. The storage ring was operating in 2/3 fill mode with a typical current of 200 mA after refill. Measurements of crystalline TMAI were carried out at 28, 50, and 150 K, and room temperature; TMAI was milled and desiccated, and a pellet of 13 mm in diameter and 1 mm in thickness containing about 50 mg of TMAI and 200 mg of boron nitride was used to collect the x-ray-absorption spectra. Three spectra were recorded and averaged for each temperature. A 0.1 M  $\Gamma^-$  aqueous solution was prepared by dissolving the appropriate amount of TMAI in deionized water. The solution was kept in a cell with Kapton windows and a 1.5 cm Teflon spacer. Also in this case three spectra were recorded and averaged.

### III. RESULTS AND DISCUSSION

In order to understand the effect of double-electron excitations on the  $\Gamma^- K$  edge, we have collected the XAS spectrum of crystalline TMAI at different temperatures. TMAI has been chosen since the first coordination shells around the iodine ion, up to about 3.82 Å, consist only of hydrogen atoms of the methyl groups.<sup>31</sup> In particular, the  $\Gamma^-$  ion has close contact with four H atoms at 3.21 Å while the next coordination shells are composed of eight H atoms at 3.43 Å, eight H atoms at 3.59 Å, and four H atoms at 3.79 Å. The first C atoms of the methyl groups lie at a distance of 3.82 Å from the  $\Gamma^-$  ion while six I-I contacts are present at 5.74 Å. The crystallographic structure of the TMAI compound is shown in Fig. 1.<sup>31</sup>

Crystals of highly symmetrical molecules often undergo solid-solid phase transitions, which are associated with changes in molecular rotational freedom. Using nuclear magnetic resonance (NMR) it was observed that rotation of methyl groups about their  $C_3$  axes, a more complex internal motion, isotropic rotation of the whole tetramethylammonium ion, and finally lattice diffusion could occur with increasing temperature.<sup>32</sup> For TMAI, <sup>2</sup>H NMR experiments

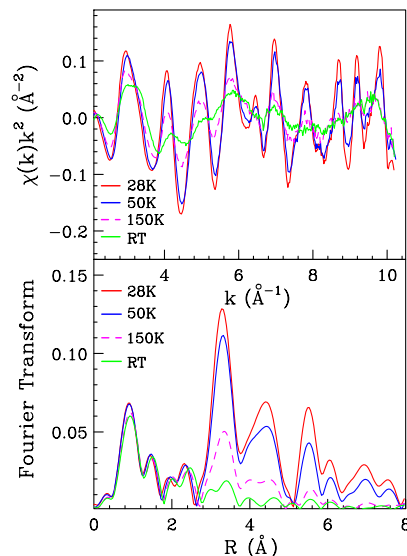


FIG. 2. (Color online) Upper panel: EXAFS signals of TMAI at 28, 50, and 150 K, and room temperature. Lower panel: Non-phase-shift corrected FTs of the 28, 50, and 150 K, and room temperature. TMAI EXAFS spectra extracted with a three-segmented cubic spline.

have shown the presence of a rigid lattice up to 150 K; after this temperature a pseudoisotropic line shape begins to appear and finally becomes the only line shape at 220 K, thus indicating the onset of a  $n$ -body rotation motion.<sup>32</sup>

The  $K$ -edge EXAFS spectra of TMAI at 28, 50, and 150 K, and room temperature are compared in the upper panel of Fig. 2. At 28 K the EXAFS signal is dominated by the single- and multiple-scattering structural contributions associated with the methyl groups in the first shells and with the iodine atoms at 5.74 Å. When the temperature is raised at 50 K, a clear thermal effect is visible as the frequency of the EXAFS oscillation is identical to that of the 28 K spectrum while the amplitude is slightly smaller. At 150 K, due to the onset of the rotational motions, the structural contribution becomes much smaller and the high-frequency components are washed out from the spectrum. This is quite evident for  $k$  values higher than 8 Å<sup>-1</sup> where the frequency of the 28 and 150 K spectra are quite different. At RT, due to the increased molecular rotational freedom, the structural contribution to the EXAFS becomes negligible and the spectrum is largely dominated by the opening of double-electron excitation channels. Note that the structural oscillations of the 28 K spectrum are quite different from the features of the room-temperature data and the diversity of the two spectra is not a pure thermal damping effect. In particular, the two spectra show the presence of features which vary both in intensity and frequency in the energy region below 8 Å<sup>-1</sup>. To be sure that the hydrogen atoms provide a negligible structural contribution to the low-energy region of the room-temperature TMAI spectrum, it is useful to compare the Fourier transform (FT) moduli of the 28, 50, and 150 K, and room-temperature TMAI EXAFS spectra extracted with a conventional three-segmented cubic spline. The FTs have been calculated with a  $k^2$  weight in the interval  $k=2.3-13.5$  Å<sup>-1</sup> with no phase-shift correction applied. The results are shown

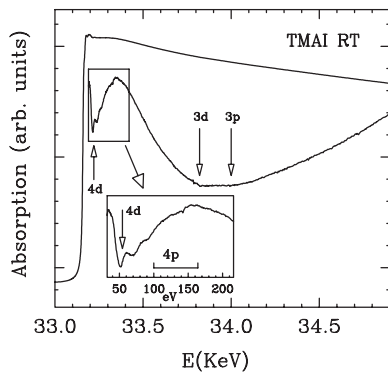


FIG. 3. Raw  $I^-$   $K$ -edge x-ray-absorption spectrum of TMAI at room temperature. The onsets of several double-electron excitation channels are indicated by the vertical arrows.

in the lower panel of Fig. 2. In the 28 K FT spectrum there are several peaks in the region between 3.3 and 8.0 Å which are associated with the different coordination shells around the  $I^-$  ion. In addition, a prominent peak is visible around 1 Å which cannot be assigned to any structural origin. When the temperature is increased, all of the structural peaks become less intense due to the thermal effect while the amplitude of the peak at 1 Å remains equal, thus demonstrating that this low-frequency peak is due to the existence of multielectron excitation channels and therefore it is not influenced by the temperature. Note that the low-distance peak is by far the most intense in the room-temperature FT while all of the other peaks in the distance range of possible structural contributions are below the experimental noise. This is a strong indication that at room temperature the structural contribution is almost negligible and the x-ray-absorption spectrum of TMAI could provide a direct experimental determination of the  $I^-$  atomic background.

The raw  $K$ -edge x-ray-absorption data of TMAI at room temperature are shown in Fig. 3. Background anomalies are quite evident in the magnified spectrum that reports the absorption excess calculated by subtracting, from the absorption spectrum, an average decay fitted in the EXAFS region. As already observed in the XAS spectrum of gaseous HI,<sup>27</sup> the increase in the absorption coefficient in the region from 50 to 250 eV above the edge is associated with the openings of additional excitations of  $4d$  and  $4p$  electrons. Moreover, clear slope changes are visible in the EXAFS region around 33 800 and 34 000 eV which are associated with the opening of the  $1s3d$  and  $1s3p$  double-electron excitations. This spectrum can be compared with the x-ray-absorption cross section of the HI gas, shown in Fig. 1 of Ref. 27. The feature at about 33 230 eV, which is associated with the opening of the  $1s4d$  channel, is present in both spectra and shows a similar trend, apart from details of multiplet structures. Moreover, the energy position and the intensity of the features associated with the double-electron excitations ( $1s3d$  and  $1s3p$ ) are almost identical in the TMAI and HI spectra because they involve deep core orbitals that are little affected by chemical bonding. Conversely, the low-energy region of the room-temperature TMAI spectrum (from the edge up to about 50 eV, see upper panel of Fig. 4) reveals the presence of structured features which are not present in the HI absorp-

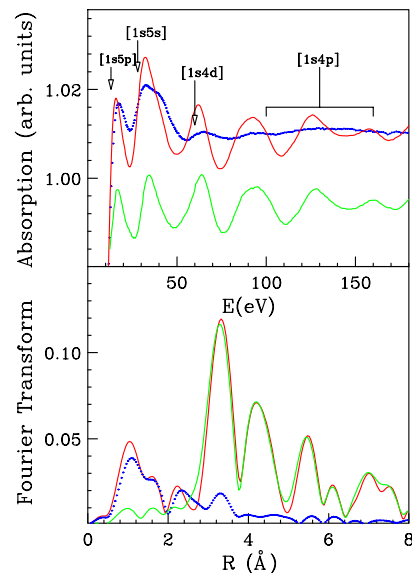


FIG. 4. (Color online) Upper panel: Normalized  $K$ -edge absorption spectra of crystalline TMAI at 28 K [red line (dark gray)] and at room temperature (blue dotted line). Arrows refer to the energy position of multielectron excitations. The last curve [green line (light gray)] is the 28 K TMAI EXAFS spectrum obtained using the room-temperature spectrum as atomic background. Lower panel: Non-phase-shift corrected FTs of the room temperature (blue dotted line) and 28 K [red line (dark gray)] TMAI EXAFS spectra extracted with a three-segmented cubic spline. The green (light gray) line is the FT of the 28 K TMAI EXAFS spectrum obtained using the room-temperature data as atomic background.

tion cross section. These additional structures are due to the onset of the  $1s5p$  and  $1s5s$  double-electron channels, and a more precise assignment of these excitations will be given below. These findings demonstrate that the shape and the onset of the valence multielectron excitations which occur in the low-energy region strongly depend on the oxidation state and the atomic bond of the photoabsorber atom. As a consequence the HI spectrum, in which the iodine atom forms a covalent bond with the hydrogen atom, does not provide a reliable description of the atomic background of the  $I^-$  ion in the XANES region. On the other hand, due to their similarity in the high-energy region (above 50 eV from the edge) either the HI or the TMAI spectrum can be used as an indicative background model to extract the EXAFS spectra of iodine compounds.

The upper panel of Fig. 4 shows the comparison between the x-ray-absorption spectra of TMAI at room temperature and 28 K. As previously observed, the former spectrum is largely dominated by the opening of double-electron excitation channels while in the latter case, due to the low thermal disorder, the structural contributions show up and are overlaid on the atomic background. A very clear picture emerges when the room-temperature spectrum is used as atomic background in the extraction of the EXAFS from the 28 K data. The resulting EXAFS spectrum is the last curve of the upper panel of Fig. 4. Note that the low-frequency contribution is completely eliminated and a well defined oscillation can be detected both in the low- and high-energy regions. The lower panel of Fig. 4 shows the comparison of the

TABLE I. Energy levels obtained from HF calculations and determined from the experimental  $K$ -edge absorption spectra of Xe, gaseous HI, and TMAI at RT. The experimental energy onsets of TMAI are measured from the  $K$ -edge energy defined as the first inflection point of the spectrum (33 158 eV). Hole states are enclosed in square brackets. All energies are in electron volts.

Config.	Xe HF <sup>a</sup>	Xe HF <sup>b</sup>	Xe exp <sup>a</sup>	HI exp <sup>c</sup>	I exp <sup>d</sup>	TMAI <sup>e</sup>
[1s5p]		10.0				12
[1s5s]		25.4				28
[1s4d]	80.6–82.3	80.4	77.6	~60	~58	60
[1s4p]	180.1	170.4	159.6	130–160		100–160
[1s4s]	238.9–241.1	221.6	226.6	160		
[1s3d]	725.5	748.1	729.6	640	~670	652
[1s3p]		996.9		960		930

<sup>a</sup>From Ref. 13.

<sup>b</sup>From Ref. 9.

<sup>c</sup>From Ref. 27.

<sup>d</sup>From Ref. 29.

<sup>e</sup>This work.

FT spectrum of the 28 K EXAFS signal extracted either with a conventional spline or using the room-temperature cross section as an effective atomic background. While the low-distance peak is present in the FT of the 28 K spectrum when a conventional spline function is used to extract the EXAFS, it completely disappears when the room-temperature spectrum is used as atomic background. On the other hand the structural peaks above 3 Å in the FT of the 28 K EXAFS extracted either with a polynomial spline or using the room-temperature spectrum as atomic background are identical. This definitely demonstrates that at room temperature the structural contribution vanishes completely and the TMAI absorption cross section provides a reliable description of the  $I^-$  atomic background.

In order to make a precise assignment of the multielectronic excitations at the  $I^-$   $K$  edge, it is useful to make a comparison between the experimental energy onsets estimated from the room-temperature TMAI spectrum with excitation energies of the isoelectronic Xe atom and with the HI molecule. The experimental energy distance between the  $K$  edge and the double-electron channel edge is the additional energy needed to perform the shake up of a shallow core electron. These values have been calculated from the difference between the onsets of the double-electron channel, defined as the zero values of the cross-section second derivative, and the  $K$ -edge threshold defined as the first inflexion point of the spectrum (at 33 158 eV). Table I compares the experimental and calculated [obtained from SCF calculations, i.e., nonrelativistic Hartree-Fock (HF)\_methods<sup>9,13</sup>] energies of the double-electron excitations in Xe and those experimentally observed in HI with our results for the  $K$  edge. The 1s5p and 1s5s edges are located in a very inconvenient region of the  $K$ -edge spectrum. Indeed, the fast increasing slope at the position of these excitations makes their precise identification quite difficult. However, the energies of these channels can be determined from the experimental data with an accuracy of ~3 eV. It is worth noting that in this case the onset of these excitation channels is clearly visible in the experimental data, at variance with the Xe data.<sup>14</sup> As

already observed by Gomilšek *et al.*<sup>14</sup> the theoretical determination of the amplitude of the 5p and 5s shake of 12% and 1.7%, respectively, is fully compatible with our experimental data. The 1s4d excitation channel is clearly visible in the raw  $K$ -edge data (see Figs. 3 and 4) and its position is in good agreement with previous determinations (see Table I). The onset of the 1s4p excitations is much less visible than the 1s4d one, and due to configuration-interaction phenomena, the spectral features must be interpreted as a superposition of a number of individual absorption edges. Therefore, even if it is difficult to make a precise assignment of this double-electron channel, the group of 4p excitations is found in the range of 100–160 eV from the main threshold. The contribution from the 1s4s double-electron excitation is expected to be negligible on the ground of comparison with Xe and Cs.<sup>14</sup> Finally, at about 652 and 930 eV, the opening of the 1s3d and 1s3p excitation channels, respectively, is clear (see Fig. 3). The agreement between the calculated and experimental values is reasonable, and it allows an unambiguous identification of the observed structures, as reported in Figs. 3 and 4.

In the last step of this investigation we checked the transferability of the  $I^-$  atomic background obtained from the room-temperature TMAI absorption cross section using this spectrum as atomic background in the extraction of the EXAFS signal of  $I^-$  in aqueous solution. Figure 5 shows the  $K$ -edge data of TMAI at room temperature and  $I^-$  in aqueous solution. As evident from the inset, the XAS spectrum of aqueous iodide solution is dominated by the structural modulations due to the solvent cage, and the multielectron excitation channels are masked. We considered two different EXAFS signals for aqueous iodide: the former using a conventional smooth polynomial spline and the latter using the room-temperature TMAI data as atomic background. Figure 6 shows the FT moduli of the aqueous iodide EXAFS spectra extracted with a conventional smooth atomic background calculated in the  $k$  range 2–9.3 Å<sup>-1</sup>. Also in this case, when a smooth polynomial spline is used as atomic background, a prominent peak appears at about 0.8 Å,

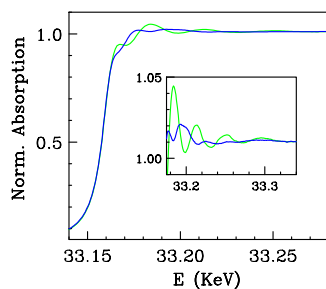


FIG. 5. (Color online) Normalized  $I^-$   $K$ -edge x-ray-absorption spectrum of TMAI at room-temperature [blue line (dark gray)] and  $I^-$  in aqueous solution [green line (light gray)]. A magnified region of the spectra is shown in the inset.

which evidently has no structural origin. On the other hand, the FT moduli of aqueous iodide show an additional peak at about 2.7 Å, which corresponds to the average distance of the first hydration shell. Figure 6 also shows the FT of aqueous iodide after subtracting the TMAI spectrum as atomic background. It can be seen that the only dominant contribution remaining after subtraction is the structural one, thus demonstrating that the nonstructural contribution has been properly removed from the spectrum.

A last remark we would like to make concerns the use of XANES spectra in the structural investigation of disordered systems. Recently, it has been shown that the quantitative analysis of XANES can provide unique information on the structural and dynamical properties of ionic solutions.<sup>33–36</sup> However, all of the available computational codes have been developed in the framework of the one-electron approximation and multielectron excitation effects are not accounted for in the theoretical calculations. In this contest a careful evaluation of the atomic background is an essential step to isolate correctly the structural signal component and to perform a reliable quantitative analysis of the XANES region. A successful attempt to use the TMAI XAS spectrum as atomic background for the XANES analysis of  $I^-$  in aqueous solution has been carried out and the results will be presented in a forthcoming paper.

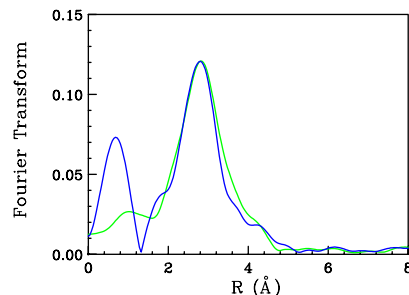


FIG. 6. (Color online) Non-phase-shift corrected FTs of  $I^-$  aqueous solution EXAFS spectra at the  $K$  edge extracted with a conventional smooth spline [blue line (dark gray)] and using the room-temperature TMAI spectrum as atomic background [green line (light gray)].

#### IV. CONCLUSIONS

In conclusion a system has been singled out which provides direct measurements of the  $I^-$  atomic background, and can be used as a reliable model in the XANES and EXAFS analysis of ionic iodide compounds. The complete sequence of multielectron excitations has been identified and the experimental energy onsets have been found to be in agreement with multielectron transitions detected at the Xe and HI  $K$  edge. It has been shown that the oxidation state and the chemical environment affect the shape of valence double-electron excitations, and the background transferability is a valid approximation only in the high-energy region of XAS spectra.

#### ACKNOWLEDGMENTS

We acknowledge the European Synchrotron Radiation Facility for provision of synchrotron-radiation facilities and we thank Michael Borowski for assistance in using beamline BM29.

\*Author to whom correspondence should be addressed. FAX: +39-06-490631; p.dangelo@caspur.it

<sup>1</sup>F. Wuillemier, J. Phys. (Paris), Colloq. **32**, C4 (1971).

<sup>2</sup>R. D. Deslattes, R. E. LaVilla, P. L. Cowan, and A. Henins, Phys. Rev. A **27**, 923 (1983).

<sup>3</sup>M. Deutsch and M. Hart, Phys. Rev. A **34**, 5168 (1986).

<sup>4</sup>M. Deutsch and M. Hart, Phys. Rev. Lett. **57**, 1566 (1986).

<sup>5</sup>M. Deutsch and M. Hart, J. Phys. B **19**, L303 (1986).

<sup>6</sup>E. Bernieri and E. Burattini, Phys. Rev. A **35**, 3322 (1987).

<sup>7</sup>M. Deutsch, G. Brill, and P. Kizler, Phys. Rev. A **43**, 2591 (1991).

<sup>8</sup>K. Zhang, E. A. Stern, J. J. Rehr, and F. Ellis, Phys. Rev. B **44**, 2030 (1991).

<sup>9</sup>M. Deutsch and P. Kizler, Phys. Rev. A **45**, 2112 (1992).

<sup>10</sup>Y. Ito, H. Nakamatsu, T. Mukoyama, K. Omote, S. Yoshikado, M. Takahashi, and S. Emura, Phys. Rev. A **46**, 6083 (1992).

<sup>11</sup>S. J. Schaphorst, A. F. Kodre, J. Ruschinski, B. Crasemann, T. Åberg, J. Tulkki, M. H. Chen, Y. Azuma, and G. S. Brown, Phys. Rev. A **47**, 1953 (1993).

<sup>12</sup>I. Arčon, A. Kodre, M. Štuhec, D. Glavič-Cindro, and W. Drube, Phys. Rev. A **51**, 147 (1995).

<sup>13</sup>Y. Ito, T. Tochio, K. Mutaguchi, H. Ohashi, N. Shigeoka, Y. Nakata, A. M. Vlaicu, T. Uruga, S. Emura, and J. P. Gomišek, Radiat. Phys. Chem. **61**, 405 (2001).

<sup>14</sup>J. P. Gomišek, A. Kodre, I. Arčon, and M. Hribar, Phys. Rev. A **68**, 042505 (2003).

<sup>15</sup>J. P. Gomišek, A. Kodre, I. Arčon, and R. Prešeren, Phys. Rev. A **64**, 022508 (2001).

<sup>16</sup>A. Kodre, I. Arčon, J. P. Gomišek, R. Prešeren, and R. Frahm, J. Phys. B **35**, 3497 (2002).

<sup>17</sup>G. Li, F. Bridges, and G. S. Brown, Phys. Rev. Lett. **68**, 1609 (1992).

- <sup>18</sup>P. D'Angelo, A. Di Cicco, A. Filipponi, and N. V. Pavel, *Phys. Rev. A* **47**, 2055 (1993).
- <sup>19</sup>J. A. Solera, J. García, and M. G. Proietti, *Phys. Rev. B* **51**, 2678 (1995).
- <sup>20</sup>P. D'Angelo, H.-F. Nolting, and N. V. Pavel, *Phys. Rev. A* **53**, 798 (1996).
- <sup>21</sup>P. D'Angelo, P.-E. Petit, and N. V. Pavel, *J. Phys. Chem. B* **108**, 11857 (2004).
- <sup>22</sup>M. Maroncelli, *J. Mol. Liq.* **57**, 1 (1993).
- <sup>23</sup>B. Bagchi and R. Biswas, *Adv. Chem. Phys.* **109**, 207 (1999).
- <sup>24</sup>D. Laage and J. T. Hynes, *Proc. Natl. Acad. Sci. U.S.A.* **104**, 11167 (2007).
- <sup>25</sup>P. D'Angelo, A. Di Nola, A. Filipponi, N. V. Pavel, and D. Roccatano, *J. Chem. Phys.* **100**, 985 (1994).
- <sup>26</sup>P. D'Angelo, A. Di Nola, M. Mangoni, and N. V. Pavel, *J. Chem. Phys.* **104**, 1779 (1996).
- <sup>27</sup>U. Buontempo, A. Di Cicco, A. Filipponi, M. Tardone, and P. Postorino, *J. Chem. Phys.* **107**, 5720 (1997).
- <sup>28</sup>P. D'Angelo and N. V. Pavel, *Phys. Rev. B* **64**, 233112 (2001).
- <sup>29</sup>J. P. Gomilšek, I. Arčon, and A. Kodre, *Acta Chim. Slov.* **53**, 18 (2006).
- <sup>30</sup>A. Filipponi, M. Borowski, D. T. Bowron, S. Ansell, A. Di Cicco, S. De Panfilis, and J.-P. Itié, *Rev. Sci. Instrum.* **71**, 2422 (2000).
- <sup>31</sup>H. Jacobs, H. Barlage, and M. Friedriszik, *Z. Anorg. Allg. Chem.* **630**, 645 (2004).
- <sup>32</sup>C. I. Ratcliffe and J. A. Ripmeester, *Can. J. Chem.* **64**, 1298 (1986).
- <sup>33</sup>P. D'Angelo, M. Benfatto, S. Della Longa, and N. V. Pavel, *Phys. Rev. B* **66**, 064209 (2002).
- <sup>34</sup>P. D'Angelo, O. M. Roscioni, G. Chillemi, S. Della Longa, and M. Benfatto, *J. Am. Chem. Soc.* **128**, 1853 (2006).
- <sup>35</sup>G. Chillemi, G. Mancini, N. Sanna, V. Barone, S. Della Longa, M. Benfatto, N. V. Pavel, and P. D'Angelo, *J. Am. Chem. Soc.* **129**, 5430 (2007).
- <sup>36</sup>P. D'Angelo, V. Migliorati, G. Mancini, V. Barone, and G. Chillemi, *J. Chem. Phys.* **128**, 084502 (2008).